frontiers in Physics

ORIGINAL RESEARCH
published: 24 March 2022
doi: 10.3389/fphy.2022.846639

Correlated Insulating Behavior in Infinite-Layer Nickelates

Y.-T. Hsu[1]*, M. Osada[2,3], B. Y. Wang[2,4], M. Berben[1], C. Duffy[1], S. P. Harvey[2,3], K. Lee[2,4], D. Li[2,3,5], S. Wiedmann[1], H. Y. Hwang[2,3] and N. E. Hussey[1,6]

[1]High Field Magnet Laboratory (HFML-EMFL) and Institute for Molecules and Materials, Radboud University, Nijmegen, Netherlands, [2]SLAC National Accelerator Laboratory, Stanford Institute for Materials and Energy Sciences, Menlo Park, CA, United States, [3]Department of Applied Physics, Stanford University, Stanford, CA, United States, [4]Department of Physics, Stanford University, Stanford, CA, United States, [5]Department of Physics, City University of Hong Kong, Hong Kong, China, [6]H. H. Wills Physics Laboratory, University of Bristol, Bristol, United Kingdom

Unlike their cuprate counterparts, the undoped nickelates are weak insulators without long-range antiferromagnetic order. Identifying the origin of this insulating behavior, found on both sides of the superconducting dome, is potentially a crucial step in the development of a coherent understanding of nickelate superconductivity. In this work, we study the normal-state resistivity of infinite-layer nickelates using high magnetic fields to suppress the superconductivity and examine the impact of disorder and doping on its overall temperature (*T*) dependence. In superconducting samples, the resistivity of Nd- and La-based nickelates continues to exhibit weakly insulating behavior with a magnitude and functional form similar to that found in underdoped electron-doped cuprates. We find a systematic evolution of the insulating behavior as a function of nominal hole doping across different rare-earth families, suggesting a pivotal role for strong electron interactions, and uncover a correlation between the suppression of the resistivity upturn and the robustness of the superconductivity. By contrast, we find very little correlation between the level of disorder and the magnitude and onset temperature of the resistivity upturn. Combining these experimental observations with previous Hall effect measurements on these two nickelate families, we consider various possible origins for this correlated insulator behavior and its evolution across their respective phase diagrams.

Keywords: superconductivity, nickelates, charge transport, metal-insulator crossover, high magnetic fields

OPEN ACCESS

Edited by:
Veerpal Singh Awana, National Physical Laboratory (CSIR), India

Reviewed by:
Jie Yuan, Institute of Physics (CAS), China
Atsushi Fujimori, Waseda University, Japan

****Correspondence:***
Y.-T. Hsu
yute.hsu@ru.nl

Specialty section:
This article was submitted to Condensed Matter Physics, a section of the journal Frontiers in Physics

Received: *31 December 2021*
Accepted: *11 February 2022*
Published: *24 March 2022*

Citation:
Hsu Y-T, Osada M, Wang BY, Berben M, Duffy C, Harvey SP, Lee K, Li D, Wiedmann S, Hwang HY and Hussey NE (2022) Correlated Insulating Behavior in Infinite-Layer Nickelates. Front. Phys. 10:846639. doi: 10.3389/fphy.2022.846639

INTRODUCTION

The recent discovery of superconductivity in the infinite-layer nickelates (ILN) [1–4] represents the culmination of a three-decade-long search to successfully dope the $3d^9$ (Ni^{1+}) configuration in a square planar geometry as a means of replicating the structural and orbital motif found in high-T_c cuprates. Unlike the cuprates, whose parent ground state is a Mott insulator with long-range antiferromagnetic (AFM) order, the undoped ILN were found to be metallic at elevated temperatures with a crossover to a weakly insulating state below approximately 100 K, at which the resistivity starts to develop a moderate upturn. While static AFM order has thus far remained undetected in the nickelates, recent resonant x-ray scattering [5] and nuclear magnetic resonance (NMR) experiments [6, 7] reported signatures consistent with fluctuating AFM paramagnon excitations. Other NMR studies, however, claimed an absence of magnetic order in the nickelates [8]. The occurrence of weakly insulating behavior at a high hole doping level, beyond the range within which superconductivity is realized, further contrasts with the correlated but nonetheless metallic ground state found in highly overdoped cuprates [9]. Numerous theoretical calculations [10–22] have indeed pointed out that the 5*d* (and possibly 4*f*) band of the rare-earth (*RE*) elements contributes a finite density of states at the Fermi level, highlighting a fundamental difference between the two $3d^9$ oxides. The sizeable negative Hall coefficient [1, 3] and the finite spectral weight at the Fermi level [23] experimentally found in undoped nickelates appear to corroborate this picture.

Despite the recent progress in understanding the low-energy electronic structure of superconducting nickelates, an understanding of the anomalous insulating behavior that is ubiquitously found in ILN is lacking. Here, we present a systematic study of the normal-state transport of two doped families of ILN—the Nd- and La-based systems—by employing high magnetic fields up to 35 T to fully suppress the superconductivity. The effect of varying the rare-earth (*RE*) element on the functional form of the insulating resistivity, as well as the impact of (hole) doping and disorder level on the transport characteristics are also investigated. By taking into account the evolution of the Hall coefficient in both systems, we arrive at a number of salient points with regards to the origin of the insulating behavior: 1) The resistive upturns at low doping are likely to be due to a partial gapping of the states derived from the *RE* ions. 2) Hole doping x is much more effective in suppressing the resistivity upturn than a decrease in disorder (as inferred from the residual resistivity ratio). 3) The upturns, though notably weaker in the superconducting samples, nevertheless persist into the superconducting regime, and show a different functional form depending on the choice of *RE*. 4) In this region of the phase diagram, the insulating behavior is more likely to be associated with the correlated 3*d* states on the Ni. 5) The field dependence of the magnetoresistance in superconducting samples appears to rule out localization or the Kondo effect as the origin of the resistive upturns. 6) The *RE* dependence on the functional form of the low-T resistivity, as well as its overall magnitude, are more reminiscent of that seen in electron-doped cuprates than in hole-doped cuprates. 7) Finally, we find that T_c in the nickelates is sensitive to the level of disorder, suggesting that superconductivity in the ILN is unconventional in nature.

MATERIALS AND METHODS

$La_{1-x}Sr_xNiO_2$ and $PrNiO_2$ thin films were grown by pulsed laser technique described in [3, 24], respectively. Electrical resistivity was measured with a four-point configuration using the ac lock-in technique, with an alternating current $I = 10\,\mu$A applied within the *ab*-plane at a frequency between 13 and 30 Hz. Static magnetic fields up to 35 T, applied parallel to the crystalline *c*-axis, were generated using a Bitter magnet at the High Field Magnet Laboratory in Nijmegen, the Netherlands.

RESULTS AND DISCUSSION

Figure 1 shows the T-dependent in-plane resistivity $\rho_{ab}(T)$ of a set of undoped RENiO$_2$ films (*RE* = La, Pr, Nd). Several key features of its normal-state resistivity are revealed in these plots. Firstly, for all films, $\rho_{ab}(T)$ undergoes a resistivity minimum ($\rho_{\min}$) at $T = T_{\min}$ that delineates the metallic regime from the insulating-like regime at lower temperatures. Secondly, the absolute values of ρ_{ab} show significant variation between samples, with the newer generation exhibiting lower absolute resistivities as well as a reduced level of disorder, as inferred from the higher $\rho_{300K}/\rho_{\min}$ ratios. As $\rho_{300K}/\rho_{\min}$ increases, $T_{\min}$ shifts to lower values, suggesting that disorder plays some role in the insulating behavior, at least in the parent compound(s). (The resistivity of $LaNiO_2$ from an early report [25] was found to be an exceptionally low yet its $\rho_{300K}/\rho_{\min}$ ratio is the lowest among all samples investigated, the origin of which is yet unclear). Thirdly, in the high-T metallic regime for $PrNiO_2$ and $NdNiO_2$, the slope $d\rho_{ab}/dT$ is found to be very similar despite a large variation in their absolute values. This suggests that the excess disorder, while increasing the impurity scattering rate (and the magnitude of ρ_{ab}), does not significantly affect the intrinsic metallic resistivity. Fourthly, the functional form of the resistive upturn over the accessible temperature range depends on the choice of *RE*. In $LaNiO_2$, for example, $\rho_{ab}(T)$ initially follows a $\log(1/T)$ behavior for $T < T_{\min}$ but then tends towards a constant value below 10 K. In contrast, $\rho_{ab}(T)$ in $PrNiO_2$ and $NdNiO_2$ $\rho_{ab}(T) \propto \log(1/T)$ down to the lowest measured temperatures. Whether or not $\rho_{ab}(T)$ in (Pr, Nd) NiO_2 saturates below ≈2 K, however, remains to be seen.

An emerging picture for the electronic structure of undoped ILN, based on recent spectroscopic studies and realistic theoretical calculations with electron interaction taken into account [15, 16, 23, 26, 27], indicates that its Fermi surface comprises a small electron pocket with a dominant character of the *RE* 5*d* band (which hybridizes with the Ni $3d_{z^2}$ band). The Ni $3d_{x^2-y^2}$ band, on the other hand, is split into the upper and lower Hubbard bands and thus does not directly contribute to the Fermi level. The Hall coefficient $R_H(T)$ in both $LaNiO_2$ and $NdNiO_2$ is found to be negative [3, 28], consistent with the notion that the 3*d* states on the Ni sites are Mott localized and that the longitudinal and Hall conductivities are dominated by the electron pocket derived from the *RE* 5*d* states. Hence, it is these states that must be responsible for the resistive upturns in the parent compounds. Secondly, in both systems, $T_{\min}$ is found to mark the onset of a marked increase in $R_H(T)$, possibly indicating some form of gap opening below $T_{\min}$. Thirdly, the fact that $\rho_{ab}(T)$ appears to saturate eventually, at least in $LaNiO_2$ (and possibly in $PrNiO_2$ too), implies that this gapping is only partial and that a finite density of states remains on the electron pocket(s) whose low-T ground state is ultimately metallic.

According to the conventional Drude transport model, the electrical conductivity σ is given by

$$\sigma = \sum_i n_i e \mu_i = \sum_i \frac{n_i e^2 \tau_i}{m_i'}, \quad (1)$$

where i denotes the distinct channel of conducting carriers, e is the elementary charge, and (μ, τ, m^*) denote the associated

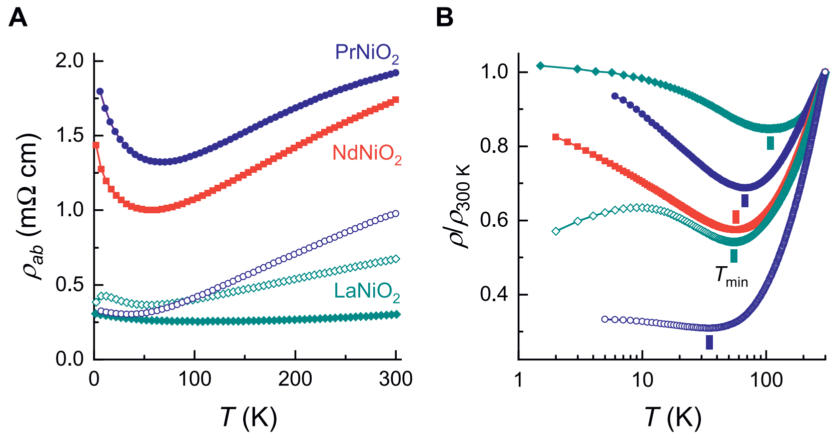

FIGURE 1 | In-plane resistivity versus temperature $\rho_{ab}(T)$ for undoped infinite-layer nickelates with selected rare earth elements. **(A)** Data from a previous generation of samples of $PrNiO_2$ [2], $NdNiO_2$ [28], and $LaNiO_2$ [25] are shown in solid points; data from a new generation of samples of $LaNiO_2$ [3] and $PrNiO_2$ (this work) in open points. **(B)** Normalized resistivity $\rho(T)/\rho_{300\ K}$ in linear-log scale with the same color code as in **(A)**. Vertical bars indicate T_{min}, the temperature at which ρ_{ab} shows a minimum.

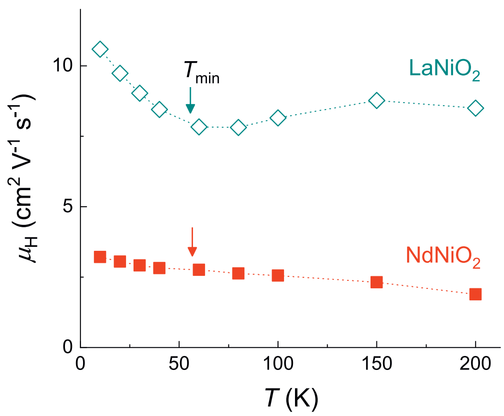

FIGURE 2 | Hall mobility μ_H of undoped $LaNiO_2$ and $NdNiO_2$. μ_H is estimated using $\mu_H = R_H/\rho$ with the Hall coefficient data R_H reported in [3, 28] and ρ as shown in **Figure 1**. The locations of T_{min} are marked by vertical arrows.

mobility, relaxation time, and effective mass, respectively. Consequently, $\rho = 1/(ne\mu) = R_H/\mu$ for a single-band metal, where $R_H = \frac{1}{ne}$ is the Hall coefficient. From **Eq. 1**, it can be seen that a reduction of conductivity (i.e. a metal-insulator transition) can be caused by a reduction of n (loss of carrier) or τ (increased scattering rate), an increase in m^* (effective mass enhancement), or a combination of these factors. For simplicity, here we estimate the carrier mobility using the measured R_H, known as the Hall mobility $\mu_H = R_H/\rho$ for undoped $LaNiO_2$ and $NdNiO_2$, for which the single-band picture is most likely to apply. As shown in **Figure 2**, both $LaNiO_2$ and $NdNiO_2$ show a relatively unchanged μ_H above T_{min}, below which μ_H increases moderately. Crucially, the increase in μ_H below T_{min} indicates that the increase in ρ below T_{min} is not related to a reduction of mobility (i.e. a change in τ/m^*), but is most likely caused by a reduction in n. The minimization of R_H at low T as x approaches 0.20, at which T_{min} and $\rho_0 - \rho_{min}$ are most suppressed (see **Figure 4**) further supports this scenario. Possible candidates responsible for the loss of carriers below T_{min} include the emergence of a secondary order parameter (e.g. magnetic, charge, or stripe order), the opening of a pseudogap that partially depletes the density of states at the Fermi level [29], or a transfer of spectral weight to higher energy [30, 31].

With hole-doping, the situation evolves in a systematic fashion. In $Nd_{1-x}Sr_xNiO_2$, we revealed previously by destroying superconductivity with a large magnetic field, that the resistivity upturn, though persisting throughout the doping range of superconductivity, is progressively suppressed, essentially vanishing as x approaches the edge of the superconducting dome $x_c \approx 0.225$ [32]. Here, we examine the evolution of the low-T resistivity in $La_{1-x}Sr_xNiO_2$ in the field-induced normal state for $0.15 \leq x \leq 0.20$, i.e. across much of the superconducting doping range [3]. A contrasting behavior manifests in the functional form of $\rho_{ab}(T)$ below T_c, as shown in **Figure 3**. Similar to the undoped compound, $\rho_{ab}(T)$ in the field-induced normal state of superconducting $La_{1-x}Sr_xNiO_2$ exhibits an initial $\log(1/T)$-behavior followed by a leveling off as $T \to 0$. The magnitude of the resistive upturn decreases as x increases from 0.15 to 0.18, after which it again increases at $x = 0.20$.

The overall magnitude of the resistive upturn, on the order of 10% between 0.5 K and T_{min}, is considerably smaller than that observed in the underdoped hole-doped cuprates ($\gtrsim$ 100%) [33, 34, 35] but is comparable with that reported in the electron-doped cuprates $RE_{2-x}Ce_xCuO_4$ below optimal doping [36–38]. A direct comparison of the low-T resistivities in the ILN and $RE_{2-x}Ce_xCuO_4$ is shown in **Figure 3C**. Intriguingly, the functional form of the low-T resistivity in $RE_{2-x}Ce_xCuO_4$ also

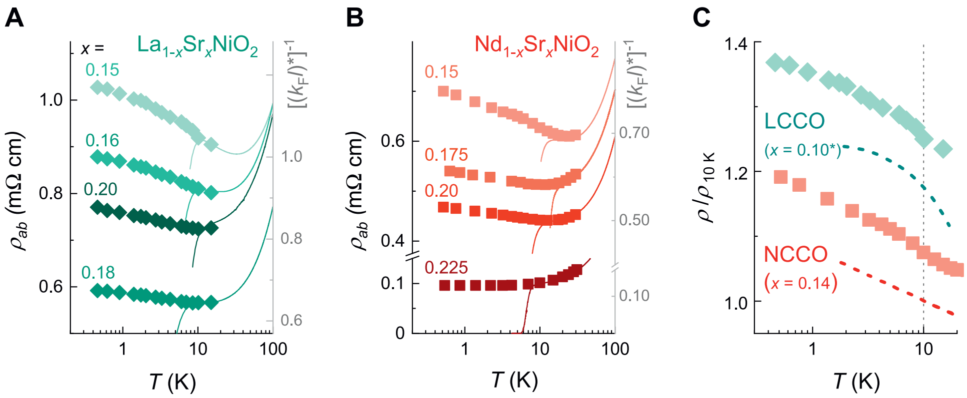

FIGURE 3 | Normal-state resistivity of superconducting nickelates at low temperatures. **(A)** $\rho_{ab}(T)$ of $La_{1-x}Sr_xNiO_2$ and **(B)** $Nd_{1-x}Sr_xNiO_2$ [32] thin films with $0.15 \leq x \leq 0.20$ measured at zero applied magnetic field (lines) and at 35 T (solid points). Magnetic field is applied along the crystalline c-axis. Right axis shows the estimates of $(k_F l)^{-1}$ assuming a two-dimensional free electron model (see main text for details). **(C)** Comparison of resistivity normalized by its 10 K value in the field-induced normal state, $\rho/\rho_{10\,K}$, for selected hole-doped nickelates (x = 0.15) and electron-doped cuprates below optimal dopings as specified. LCCO: representative ρ_{ab}(T) $La_{2-x}Ce_xCuO_4$ measured at $\mu_0 H$ = 10 T [38]. NCCO: representative ρ_{ab}(T) $Nd_{2-x}Ce_xCuO_4$ measured at $\mu_0 H$ = 14 T [37]. Note that the temperature axes are shown in log-scale and a vertical shift is applied to **(C)** for clarity. For LCCO, a rescaling factor of 0.50 is applied to the change in $\rho/\rho_{10\,K}$, which does not affect the functional form of $\rho(T)$.

depends on the RE elements in a similar manner to what is seen in the ILN. For $La_{2-x}Ce_xCuO_4$ (LCCO, x = 0.08) $\rho_{ab}(T)$ appears to saturate below 4 K, while for $Nd_{2-x}Ce_xCuO_4$ (NCCO, x = 0.14), $\rho_{ab}(T) \propto \log(1/T)$ down to the lowest measured temperature. This close alignment to the experimental situation in the n-doped cuprates is curious, but may simply be a consequence of the way in which carriers are doped into each system. In the cuprates, doped holes sit preferentially on the O sites while doped electrons reside on the Cu sites [39]. In the ILN, it is thought that the carriers are also introduced directly into the $3d_{x^2-y^2}$ orbital on the Ni sites [40]. At the same time, the similarities found in the low-T $\rho_{ab}(T)$ behavior of the ILN (for which no long-range AFM order exists at half-filling) and the n-doped cuprates suggests that the resistive upturns in the latter are not necessarily caused by short-range spin correlations, as is believed to be the case for the p-doped cuprates.

The evolution of $R_H(T)$ with doping in both ILN families is qualitatively the same, with a gradual reduction in the overall magnitude of R_H culminating in a crossover from negative to positive $R_H(0)$ (the Hall coefficient in the low-T limit) around optimal doping [1, 3]. In any two-band metallic system, the sign of $R_H(0)$ reflects the sign of the most mobile carriers. Hence, the observed sign change signals a delocalization of the 3d hole states on the Ni sites with hole-doping until eventually, they become the most mobile carriers in each system. Nevertheless, the fact that $\rho_{ab}(T)$ continues to exhibit a logarithmic divergence (at least in $Nd_{1-x}Sr_xNiO_2$) implies that these carriers are also prone to some form of localization, however weak. (Note that $R_H(T)$ exhibits no upturns within the superconducting doping range, and so it is unlikely that the resistive upturns here are due to partial gapping).

It was noted early on that the insulator-to-metal crossover in the cuprates occurs at a threshold value of $k_F\ell > 10$ for both the hole- [35] and electron-doped [36] compounds, far higher than the usual criterion $k_F\ell \approx 1$. Assuming that the suppression of the resistive upturn in $Nd_{0.775}Sr_{0.225}NiO_2$ reflects a metallic ground state and using the two-dimensional free electron model [35]:

$$\rho_{ab}/d = h/\left(e^2 k_F \ell\right), \quad (2)$$

where d is the c-axis lattice spacing, k_F is the Fermi wavevector, and l is the electronic mean free path, we find a threshold $k_F l \approx 2 - 10$ for low-T metallicity in the ILN. We note, however, that the assumption of a single-band, 2D Fermi surface is likely not valid for the entire series of hole-doped nickelates (due to the expected presence of a 3D electron pocket derived from the 5d band of RE elements); therefore the estimates of $k_F l$ here should be interpreted with caution.

Several proposals have been put forward to explain the anomalous upturn in the normal-state resistivity in the nickelates [31, 41, 42]. Two well-known mechanisms to produce a logarithmically diverging resistivity at low T are weak localization due to disorder [43, 44] and Kondo scatterings due to magnetic impurities [14, 45]. In both circumstances, however, a strong negative magnetic-field dependence of the insulating resistivity is expected, which is not observed in the nickelates. Moreover, a monotonic suppression of the insulating behavior with decreasing residual resistivity, expected for a localization-driven origin, is not seen (**Figure 4**) while the re-entrant insulating behavior found at high dopings also cannot be naturally explained by a Kondo-like mechanism.

In order to gain further insights into the origin of the resistive upturns, we have examined the impact of disorder and doping on the insulating characteristics in the ILN, namely the onset temperature (T_{min}) and the size of the resistivity upturn ($\rho(T \to 0) - \rho(T_{min})$), denoted as $\rho_0 - \rho_{min}$), as shown in **Figure 4**. We find no clear correlations

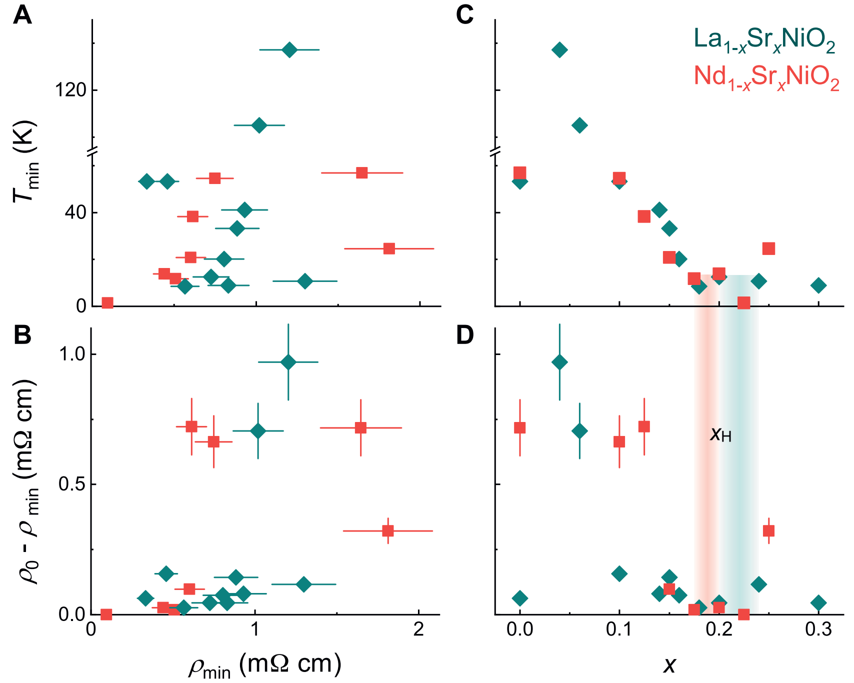

FIGURE 4 | Effect of disorder and hole doping on the insulating characteristics. **(A)** Onset temperature of the resistive upturn (T_{min}) and **(B)** its absolute magnitude ($\rho_0 - \rho_{min}$) versus the normal-state resistivity at its minimum (ρ_{min}) for $La_{1-x}Sr_xNiO_2$ (diamonds) and $Nd_{1-x}Sr_xNiO_2$ (squares). **(C)** T_{min} and **(D)** $\rho_0 - \rho_{min}$ versus the hole doping x given by the nominal Sr level. Color shades indicate the doping levels x_H at which the Hall coefficients change sign at low temperatures (10 K) [3, 28]. Error bars of 15% due to geometric uncertainties are applied to the resistivity data.

between T_{min} and ρ_{min} (**Figure 4A**) nor between $\rho_0 - \rho_{min}$ and ρ_{min} (**Figure 4B**), for both $Nd_{1-x}Sr_xNiO_2$ and $La_{1-x}Sr_xNiO_2$. Meanwhile, T_{min} and $\rho_0 - \rho_{min}$ both appear to collapse near $x = 0.20$ (**Figures 4C,D**), though deviations from the overall trends are visible both at zero doping and at the highest dopings. Notably, while T_{min} and $\rho_0 - \rho_{min}$ are gradually suppressed with improved sample quality (**Figure 1B**), varying x is seen as much more effective in suppressing the insulating behavior, suggesting that it is sensitive to carrier screenings and primarily driven by electron correlation effects. A number of non-Fermi-liquid models have been proposed to explain the anomalous insulating behavior seen in underdoped cuprates, including those based on the marginal Fermi liquid [46], the 2D Luttinger liquid [47] and the polaronic Bose liquid [48] model. The relevance of these more exotic models to the ILN, whose distinction from the (hole-doped) cuprates has become increasingly established, remains to be examined.

Lastly, we examine the impact of disorder on the critical temperature of superconducting nickelates. **Figure 5** shows a compilation of $Nd_{0.8}Sr_{0.2}NiO_2$ resistivity data reported to date [1, 28, 32, 49–53]. A large difference in the absolute values of ρ_{ab} is found, with ρ_{ab}(300 K) ranging from ~ 0.1–6.75 mΩ cm for nominally the same samples. Meanwhile, the agreement in the normalized resistivity $\rho/\rho_{300\ K}$ is much better across different reports, as shown in **Figure 5B**, with a good overlap found in 6 out of 9 traces. This suggests the discrepancy in the absolute resistivities arises from geometric uncertainties. Importantly, we find that T_c depends strongly on the residual resistivity ratio, defined as $\rho_{300\ K}/\rho_{20\ K}$, with T_c increasing from ≈5 K to over 12.5 K as $\rho_{300\ K}/\rho_{20\ K}$ increases. Such a strong dependence of T_c with respect to the level of disorder points to an unconventional nature of the superconductivity in the nickelates, and hints at a possible further increase in T_c with improved sample quality.

CONCLUSION

In summary, by suppressing superconductivity with high magnetic fields, we find the unusual resistivity upturn in the undoped infinite-layer nickelates persists into the superconducting regime and appears to be maximally suppressed near $x = 0.20$ in both La- and Nd-based systems. The resilience of the resistivity upturn against magnetic fields rules out localization and Kondo effect as its origin, and points to a partial gapping of the states with dominant *RE* 5*d* character as its cause at low doping as supported by Hall mobility analysis. In the superconducting doping range, the resistive upturn is found to be highly reminiscent in both its functional form and its overall magnitude to that found in electron-doped cuprates, which suggests the insulating behaviour is associated with the correlated Ni 3*d* states. While disorder has only a minor impact on the insulating behavior, the robustness of

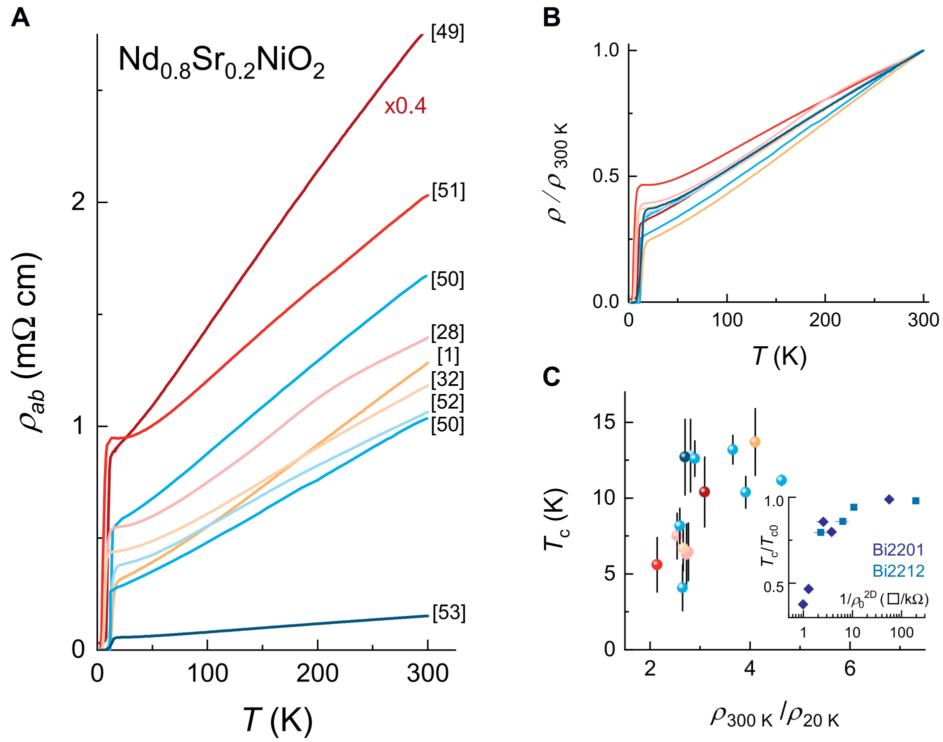

FIGURE 5 | Impact of disorder on the critical temperature T_c of $Nd_{0.8}Sr_{0.2}NiO_2$. **(A)** A compilation of representative resistivity data on $Nd_{0.8}Sr_{0.2}NiO_2$ films reported in [1, 28, 32, 49–53]. Data reported in [49] is rescaled by a factor of 0.4 for clarity. **(B)** Normalized resistivity $\rho/\rho_{300\ K}$ of data shown in **(A)**. **(C)** T_c versus residual resistivity ratio $\rho_{300\ K}/\rho_{20\ K}$. T_c is defined as the midpoint of the resistive superconducting transition and the error bars reflect the 10–90% transition width. The same color code is applied to all panels. Inset: The impact of disorder on T_c of Bi-based cuprates. For both $Bi_2(Sr, La)_2CuO_{6+\delta}$ (Bi2201) and $Bi_2Sr_2CaCu_2O_{8+\delta}$ (Bi2212), T_c is found to be strongly reduced from the optimized value T_{c0} with an increase in residual resistivity per CuO_2 plane (ρ_0^{2D}, similar to that found in $Nd_{0.8}Sr_{0.2}NiO_2$. Data reproduced from [54].

superconductivity is strongly affected by the level of disorder, pointing towards the unconventional nature of nickelate superconductivity.

DATA AVAILABILITY STATEMENT

The original contributions presented in the study are included in the article/Supplementary Material, further inquiries can be directed to the corresponding author.

AUTHOR CONTRIBUTIONS

YTH, HYH and NEH conceived the experiments. MO, BW, SH, KL, and DL grew and prepared the thin-film samples. YTH, MB, CD, and SW performed the resistivity measurements. YTH and NEH analyzed the data and wrote the manuscript with contribution from all authors.

FUNDING

This work was supported by the Netherlands Organisation for Scientific Research (NWO) grant No. 16METL01 “Strange Metals” and the European Research Council (ERC) under the European Union’s Horizon 2020 research and innovation programme (Grant Agreement No. 835279-Catch-22). The work at SLAC/Stanford is supported by the US Department of Energy, Office of Basic Energy Sciences, Division of Materials Sciences and Engineering, under contract number DE-AC02-76SF00515; and the Gordon and Betty Moore Foundations Emergent Phenomena in Quantum Systems Initiative through grant number GBMF9072 (synthesis equipment).

ACKNOWLEDGMENTS

We acknowledge the support of the HFML-RU/NWO, a member of the European Magnetic Field Laboratory (EMFL).

REFERENCES

1. Li D, Lee K, Wang BY, Osada M, Crossley S, Lee HR, et al. Superconductivity in an Infinite-Layer Nickelate. *Nature* (2019) 572:624–7. doi:10.1038/s41586-019-1496-5
2. Osada M, Wang BY, Goodge BH, Lee K, Yoon H, Sakuma K, et al. A Superconducting Praseodymium Nickelate with Infinite Layer Structure. *Nano Lett* (2020) 20:5735–40. doi:10.1021/acs.nanolett.0c01392
3. Osada M, Wang BY, Goodge BH, Harvey SP, Lee K, Li D, et al. Nickelate Superconductivity without Rare-Earth Magnetism: (La,Sr)NiO_2. *Adv Mater* (2021) 33:2104083. doi:10.1002/adma.202104083
4. Zeng SW, Li CJ, Chow LE, Cao Y, Zhang ZT, Tang CS, et al. *Superconductivity in Infinite-Layer Lanthanide Nickelates* (2021). preprints, arXiv:2105.13492.
5. Lu H, Rossi M, Nag A, Osada M, Li DF, Lee K, et al. Magnetic Excitations in Infinite-Layer Nickelates. *Science* (2021) 373:213–6. doi:10.1126/science.abd7726
6. Cui Y, Li C, Li Q, Zhu X, Hu Z, Yang Y-f., et al. NMR Evidence of Antiferromagnetic Spin Fluctuations in Nd 0.85Sr0.15 NiO_2. *Chin Phys. Lett.* (2021) 38:067401. doi:10.1088/0256-307x/38/6/067401
7. Lin H, Gawryluk DJ, Klein YM, Huangfu S, Pomjakushina E, von Rohr F, et al. *Universal Spin-Glass Behavior in Bulk La NiO_2, $PrNiO_2$, and $NdNiO_2$.* Preprints (2021). arXiv:2104.14324.
8. Zhao D, Zhou YB, Fu Y, Wang L, Zhou XF, Cheng H, et al. Intrinsic Spin Susceptibility and Pseudogaplike Behavior in Infinite-Layer $LaNiO_2$. *Phys Rev Lett* (2021) 126:197001. doi:10.1103/physrevlett.126.197001
9. Nakamae S, Behnia K, Mangkorntong N, Nohara M, Takagi H, Yates SJC, et al. Electronic Ground State of Heavily Overdoped nonsuperconducting La_2−xSrx CuO_4. *Phys Rev B* (2003) 68:100502. doi:10.1103/physrevb.68.100502
10. Lee K-W, Pickett WE. Infinite-layer $LaNiO_2$: Ni^{1+} is not Cu^{2+}. *Phys Rev B* (2004) 70:165109. doi:10.1103/physrevb.70.165109
11. Nomura Y, Hirayama M, Tadano T, Yoshimoto Y, Nakamura K, Arita R. Formation of a Two-Dimensional Single-Component Correlated Electron System and Band Engineering in the Nickelate Superconductor Nd NiO_2. *Phys Rev B* (2019) 100:205138. doi:10.1103/physrevb.100.205138
12. Botana AS, Norman MR. Similarities and Differences between $LaNiO_2$ and $CaCuO_2$ and Implications for Superconductivity. *Phys Rev X* (2020) 10:011024. doi:10.1103/physrevx.10.011024
13. Wu X, Di Sante D, Schwemmer T, Hanke W, Hwang HY, Raghu S, et al. Robust-wave Superconductivity of Infinite-Layer Nickelates. *Phys Rev B* (2020) 101:060504. doi:10.1103/physrevb.101.060504
14. Zhang YH, Vishwanath A. Type-II $T-J$ Model in Superconducting Nickelate $Nd_{1-x}Sr_xNiO_2$. *Phys Rev Res* (2020) 2:023112. doi:10.1103/physrevresearch.2.023112
15. Lechermann F. Late Transition Metal Oxides with Infinite-Layer Structure: Nickelates versus Cuprates. *Phys Rev B* (2020) 101:081110. doi:10.1103/physrevb.101.081110
16. Been E, Lee WS, Hwang HY, Cui Y, Zaanen J, Devereaux T, et al. Electronic Structure Trends across the Rare-Earth Series in Superconducting Infinite-Layer Nickelates. *Phys Rev X* (2021) 11:011050. doi:10.1103/physrevx.11.011050
17. Karp J, Botana AS, Norman MR, Park H, Zingl M, Millis A. Many-body Electronic Structure of $NdNiO_2$ and $CaCuO_2$. *Phys Rev X* (2020) 10:021061. doi:10.1103/physrevx.10.021061
18. Sakakibara H, Usui H, Suzuki K, Kotani T, Aoki H, Kuroki K. Model Construction and a Possibility of Cupratelike Pairing in a New D^9 Nickelate Superconductor (Nd, Sr)NiO_2. *Phys Rev Lett* (2020) 125:077003. doi:10.1103/physrevlett.125.077003
19. Adhikary P, Bandyopadhyay S, Das T, Dasgupta I, Saha-Dasgupta T. Orbital-selective Superconductivity in a Two-Band Model of Infinite-Layer Nickelates. *Phys Rev B* (2020) 102:100501. doi:10.1103/physrevb.102.100501
20. Wang Y, Kang CJ, Miao H, Kotliar G. Hund's Metal Physics: From $SrNiO_2$ to $LaNiO_2$. *Phys Rev B* (2020) 102:16118. doi:10.1103/physrevb.102.161118
21. Liu Z, Xu C, Cao C, Zhu W, Wang ZF, Yang J. Doping Dependence of Electronic Structure of Infinite-Layer $NdNiO_2$. *Phys Rev B* (2021) 103:045103. doi:10.1103/physrevb.103.045103
22. Higashi K, Winder M, Kunes J, Hariki A. Core-level X-ray Spectroscopy of Infinite-Layer Nickelate: LDA + DMFT Study. *Phys Rev X* (2021) 11:041009. doi:10.1103/physrevx.11.041009
23. Chen Z, Osada M, Li D, Been EM, Chen SD, Hashimoto M, et al. *Electronic Structure of Superconducting Nickelates Probed by Resonant Photoemission Spectroscopy* (2021). *preprints*, arXiv:2106.03963.
24. Osada M, Wang BY, Lee K, Li D, Hwang HY. Phase Diagram of Infinite Layer Praseodymium Nickelate Pr1−xSrx NiO_2 Thin Films. *Phys Rev Mater* (2020) 4:121801. (R). doi:10.1103/physrevmaterials.4.121801
25. Ikeda A, Krockenberger Y, Irie H, Naito M, Yamamoto H. Direct Observation of Infinite NiO2planes in $LaNiO_2$ films. *Appl Phys Express* (2016) 9:061101. doi:10.7567/apex.9.061101
26. Hepting M, Li D, Jia CJ, Lu H, Paris E, Tseng Y, et al. Electronic Structure of the Parent Compound of Superconducting Infinite-Layer Nickelates. *Nat Mater* (2020) 19:381–5. doi:10.1038/s41563-019-0585-z
27. Goodge BH, Li D, Lee K, Osada M, Wang BY, Sawatzky GA, et al. Doping Evolution of the Mott-Hubbard Landscape in Infinite-Layer Nickelates. *Proc Natl Acad Sci USA* (2021) 118:e2007683118. doi:10.1073/pnas.2007683118
28. Li D, Wang BY, Lee K, Harvey SP, Osada M, Goodge BH, et al. Superconducting Dome in $Nd_{1-x}Sr_xNiO_2$ Infinite Layer Films. *Phys Rev Lett* (2020) 125:027001. doi:10.1103/physrevlett.125.027001
29. Laliberte F, Tabis W, Badoux S, Vignolle B, Destraz D, Momono N, et al. Origin of the Metal-To-Insulator Crossover in Cuprate Superconductors. *preprints* (2016). arXiv:1606.04491.
30. Hussey NE, Takenaka K, Takagi H. Universality of the Mott-Ioffe-Regel Limit in Metals. *Philos Mag* (2004) 84:2847–64. doi:10.1080/14786430410001716944
31. Singh N. *A Road-Map of Nickelate Superconductivity* (2019). preprints, arXiv:1909.07688.
32. Hsu Y-T, Wang BY, Berben M, Li D, Lee K, Duffy C, et al. Insulator-to-metal Crossover Near the Edge of the Superconducting Dome in Nd1−xSrx NiO_2. *Phys Rev Res* (2021) 3:L042015. doi:10.1103/physrevresearch.3.l042015
33. Ando Y, Boebinger GS, Passner A, Kimura T, Kishio K. Logarithmic Divergence of Both In-Plane and Out-Of-Plane Normal-State Resistivities of Super conducting La_2−xSrx CuO_4 in the Zero-Temperature Limit. *Phys Rev Lett* (1995) 75:4662–5. doi:10.1103/physrevlett.75.4662
34. Boebinger GS, Ando Y, Passner A, Kimura T, Okuya M, Shimoyama J, et al. Insulator-to-Metal Crossover in the Normal State of La_2−xSrx CuO_4 Near Optimum Doping. *Phys Rev Lett* (1996) 77:5417–20. doi:10.1103/physrevlett.77.5417
35. Ono S, Ando Y, Murayama T, Balakirev FF, Betts JB, Boebinger GS. Metal-to-Insulator Crossover in the Low-Temperature Normal State of Bi_2 Sr_2−xLax CuO_6+δ. *Phys Rev Lett* (2000) 85:638–41. doi:10.1103/physrevlett.85.638
36. Fournier P, Mohanty P, Maiser E, Darzens S, Venkatesan T, Lobb CJ, et al. Insulator-Metal Crossover Near Optimal Doping in Pr_2−xCex CuO_4: Anomalous Normal-State Low Temperature Resistivity. *Phys Rev Lett* (1998) 81:4720–3. doi:10.1103/physrevlett.81.4720
37. Li SY, Mo WQ, Chen XH, Xiong YM, Wang CH, Luo XG, et al. Low-temperature Transport Properties of Nd_2−xCex CuO_4+δ: Metal-Insulator Crossover in the Overdoped Regime. *Phys Rev B* (2002) 65:224515. doi:10.1103/physrevb.65.224515
38. Sarkar T, Mandal PR, Higgins JS, Zhao Y, Yu H, Jin K, et al. Fermi Surface Reconstruction and Anomalous Low-Temperature Resistivity in Electron-Doped La_2−xCex CuO_4. *Phys Rev B* (2017) 96:155449. doi:10.1103/physrevb.96.155449
39. Armitage NP, Fournier P, Greene RL. Progress and Perspectives on Electron-Doped Cuprates. *Rev Mod Phys* (2010) 82:2421–87. doi:10.1103/revmodphys.82.2421
40. Botana AS, Kwan-Woo Lee KW, Norman MR, Pardo V, Pickett WE. Low Valence Nickelates: Launching the Nickel Age of Superconductivity. *preprints* (2021) 10. arXiv:2111.01296.
41. Zhang GM, Yang YF, Zhang FC. Self-doped Mott Insulator for Parent Compound of Nickelate Superconductors. *Phys Rev B* (2020) 101:020501. doi:10.1103/physrevb.101.020501
42. Wang Z, Zhang G-M, Yang Y-f., Zhang F-C. Distinct Pairing Symmetries of Superconductivity in Infinite-Layer Nickelates. *Phys Rev B* (2020) 102:220501. doi:10.1103/physrevb.102.220501

43. Rullier-Albenque F, Alloul H, Tourbot R, Proust C. Disorder and Transport in Cuprates: Weak Localization and Magnetic Contributions. *Phys Rev Lett* (2001) 87:157001. doi:10.1103/physrevlett.87.157001
44. Rullier-Albenque F, Alloul H, Balakirev F, Proust C. Disorder, Metal-Insulator Crossover and Phase Diagram in High-T C Cuprates. *Europhys Lett* (2008) 81: 37008. doi:10.1209/0295-5075/81/37008
45. Dagan Y, Barr MC, Fisher WM, Beck R, Dhakal T, Biswas A, et al. Origin of the Anomalous Low Temperature Upturn in the Resistivity of the Electron-Doped Cuprate Superconductors. *Phys Rev Lett* (2005) 94:057005. doi:10.1103/PhysRevLett.94.057005
46. Kotliar G, Abrahams E, Ruckenstein AE, Varma CM, Littlewood PB, Schmitt-Rink S. Long-wavelength Behavior, Impurity Scattering and Magnetic Excitations in a Marginal Fermi Liquid. *Europhys Lett* (1991) 15:655–60. doi:10.1209/0295-5075/15/6/016
47. Anderson PW, Ramakrishnan TV, Strong S, Clarke DG. Coherence and Localization in 2D Luttinger Liquids. *Phys Rev Lett* (1996) 77:4241–4. doi:10.1103/physrevlett.77.4241
48. Alexandrov AS. Logarithmic normal State Resistivity of High-Tc Cuprates. *Phys Lett A* (1997) 236:132–6. doi:10.1016/s0375-9601(97)00714-7
49. Zeng S, Tang CS, Yin X, Li C, Li M, Huang Z, et al. Phase Diagram and Superconducting Dome of Infinite-Layer $Nd_{1x}Sr_xNiO_2$ Thin Films. *Phys Rev Lett* (2020) 125:147003. doi:10.1103/physrevlett.125.147003
50. Zeng SW, Yin XM, Li CJ, Tang CS, Han K, Huang Z, et al. *Observation of Perfect Diamagnetism and Interfacial Effect on the Electronic Structures in $Nd_{0.8}Sr_{0.2}NiO_2$ Superconducting Infinite Layers* (2021). arXiv:2104.14195
51. Gao Q, Zhao Y, Zhou X-J, Zhu Z. Preparation of Superconducting Thin Films of Infinite-Layer Nickelate $Nd_{0.8}Sr_{0.2}NiO_2$. *Chin Phys. Lett.* (2021) 38:077401. doi:10.1088/0256-307x/38/7/077401
52. Xiang Y, Li Q, Li Y, Yang H, Nie Y, Wen H-H. Physical Properties Revealed by Transport Measurements for Superconducting $Nd_{0.8}Sr_{0.2}NiO_2$ Thin Films. *Chin Phys. Lett.* (2021) 38:047401. doi:10.1088/0256-307x/38/4/047401
53. Li Y, Sun W, Yang J, Cai X, Guo W, Gu Z, et al. Impact of Cation Stoichiometry on the Crystalline Structure and Superconductivity in Nickelates. *Front Phys* (2021) 9:719534. doi:10.3389/fphy.2021.719534
54. Hobou H, Ishida S, Fujita K, Ishkado M, Kojima KM, Eisaki H, et al. Enhancement of Superconducting Critical Temperature in $Bi_2Sr_2CaCu_2O_{8+\delta}$ by Controlling Disorder outside CuO_2 Planes. *Phys Rev B* (2009) 79:064507. doi:10.1103/physrevb.79.064507

Conflict of Interest: The authors declare that the research was conducted in the absence of any commercial or financial relationships that could be construed as a potential conflict of interest.